METABOLIC FINGERPRINT OF GESTATIONAL DIABETES MELLITUS

Danuta Dudzik[1, 2], Marcin Zorawski[2], Mariusz Skotnicki[3], Wieslaw Zarzycki[4], Gabryela Kozlowska[4], Katarzyna Bibik-Malinowska[3], María Vallejo[1], Antonia García[1], Coral Barbas[1], M.Pilar Ramos[5]

[1]CEMBIO (Center for Metabolomics and Bioanalysis), Facultad de Farmacia, Universidad CEU San Pablo, Madrid, Spain; [2]Department of Pharmacology, Medical University of Bialystok, Bialystok, Poland; [3]Clinical Department of Perinatology, Public Clinic Hospital, Medical University of Bialystok, Bialystok, Poland; [4]Clinical Department of Endocrinology, Diabetology and Internal Diseases, Public Clinic Hospital, Medical University of Bialystok, Bialystok, Poland; [5]Biochemistry and Molecular Biology, Facultad de Farmacia, Universidad CEU San Pablo, Madrid, Spain.

Running title: Metabolic fingerprint of Gestational Diabetes Mellitus

Keywords: Gestational Diabetes Mellitus; Maternal Metabolism; Metabolic fingerprinting

To whom correspondence should be adressed:

Mª del Pilar Ramos Álvarez, PhD.
Facultad de Farmacia
Universidad San Pablo CEU
Ctra. Boadilla del Monte km 5,3
28668, Madrid
+34-91-3724760

pramos@ceu.es

ABSTRACT

Gestational Diabetes (GDM) is causing severe short- and long-term complications for mother, fetus or neonate. As yet, the metabolic alterations that are specific for the development of GDM have not been fully determined, which also precludes the early diagnosis and prognosis of this pathology. In this pilot study, we determine the metabolic fingerprint, using a multiplatform LC-QTOF/MS, GC-Q/MS and CE-TOF/MS system, of plasma and urine samples of 20 women with GDM and 20 with normal glucose tolerance in the second trimester of pregnancy. Plasma fingerprints allowed for the discrimination of GDM pregnant women from controls. In particular, lysoglycerophospholipids showed a close association with the glycemic state of the women. In addition, we identified some metabolites with a strong discriminative power, such as LPE(20:1), (20:2), (22:4); LPC(18:2), (20:4), (20:5); LPI(18:2), (20:4); LPS(20:0) and LPA(18:2), as well as taurine-bile acids and long-chain polyunsaturated fatty acids derivatives. Finally, we provide evidence for the implication of these compounds in metabolic routes, indicative of low-grade inflammation and altered redox-balance, that may be related with the specific pathophysiological context of the genesis of GDM. This highlights their potential use as prognostic markers for the identification of women at risk to develop severe glucose intolerance during pregnancy.

Biological Significance:

Gestational Diabetes Mellitus (GDM) is increasing worldwide and, although diabetes usually remits after pregnancy, women with GDM have a high risk of developing postpartum type 2-diabetes, particularly when accompanied by obesity. Therefore, understanding the

pathophysiology of GDM, as well as the identification of potentially modifiable risk factors and early diagnostic markers for GDM are relevant issues. In the present study, we devised a multiplatform metabolic fingerprinting approach to obtain a comprehensive picture of the early metabolic alternations that occur in GDM, and may reflect on the specific pathophysiological context of the disease. Future studies at later stages of gestation will allow us to validate the discriminant power of the identified metabolites.

Gestational Diabetes Mellitus (GDM), defined as "any degree of glucose intolerance with onset or first recognition during pregnancy" [1], is increasing worldwide and, depending on the population analyzed and on the diagnostic criteria used, its prevalence ranges from 3%-14% of all pregnancies. Despite advances in diagnosis and good maternal control [2], GDM is frequently causing short- and long-term health complications for the mother, the fetus and the neonate [3]. Furthermore, although diabetes usually remits after pregnancy, women with GDM have a high risk of developing postpartum type 2-diabetes, particularly when accompanied by obesity [4].

There is lack of international uniformity regarding the ascertainment and diagnosis of GDM. Therefore, understanding the pathophysiology of GDM, as well as the identification of potentially modifiable risk factors and early diagnostic markers for GDM are relevant issues. Contemporary "omics" approaches, in particular metabolomics, provide deeper insights in the etiopathogenesis and discovery of biomarkers of diseases. A unique and disease-specific metabolite pattern or "fingerprint" allows for deciphering biological processes, and for the identification of compounds with potential diagnostic or predictive power. A growing number of metabolomics studies aimed at uncovering the metabolic signature of type 2-diabetes [5, 6], focusing on potential biomarkers of altered glucose tolerance and onset of insulin resistance, such as branched-chain amino acids, acylcarnitines, choline-containing phospholipids and 2-hydroxybutyrate [7].

In the present study, we devised a multiplatform metabolic fingerprinting approach to obtain a comprehensive picture of the early metabolic alternations that occur in GDM, and to eventually identify potential biomarkers that predict the risk of the GDM pregnant women to develop severe

glucose intolerance that will be validated in future studies at later stages of gestation and on an independent cohort of women.

RESEARCH DESIGN AND METHODS

Study population

GDM screening was done routinely at 22-28 weeks of gestation after overnight fasting by an oral glucose tolerance test (OGTT). According to WHO-1998 criteria, GDM was defined as glucose level ≥140 mg/dl (7.8 mmol/l) after 2-h 75-g OGTT. Women known to have previous diabetes mellitus or other complications were excluded from the study. Finally, twenty caucasian women with GDM and 20 healthy caucasian pregnant women with normal glucose tolerance were matched according to week of gestation and age (22-37 years). At the day of the OGTT, venous fasting blood samples were drawn into EDTA-containing tubes and overnight urine was collected. Samples were stored at –80ºC until analysis. The study was carried out in accordance with the permission of the Bioethical Commission of the Medical University of Bialystok, Poland. Written informed consent was obtained from each participant in the study.

Biochemical analysis and indices of insulin resistance

Plasma glucose, cholesterol, LDL/HDL-cholesterol, triacylglycerols and C-reactive protein (CRP) were measured in an autoanalyzer (Cobas C111 Roche Autoanalyzer, Hoffmann-LaRoche Ltd., Basel Switzerland). Blood HbA1c was analyzed by the D-10^{TM} Hemoglobin Testing System (Bio-Rad, USA), C-peptide by an ELISA kit (Biosource International, Inc., Belgium),

and insulin with an INS-IRMA-RIA kit (DIAsource ImmunoAssays S.A., Belgium). HOMA-IR (Homeostatic Model Assessment) [8] and QUICKI (Quantitative Insulin Sensitivity Check Index) [9] indices were calculated with fasting glucose (mg/dL) and insulin (μU/mL) as described. The area under the curve (AUC-G) for glucose during the OGTT was determined by the trapezoidal method with Prism 6.0 software.

Metabolic fingerprinting

Standards for GC-MS and organic solvents were from Sigma-Aldrich (Madrid, Spain); standards and reference mass solutions for LC-MS and CE-MS were from Agilent Technologies (Madrid, Spain).

Sample preparation was done according to standard protocols [10-12]. Briefly, for LC-MS analysis, proteins were precipitated by mixing 1 volume of plasma with 3 volumes of methanol/ethanol (1:1); for GC-MS analysis, protein precipitation was performed by treatment with cold acetonitrile (1:3), followed by methoximation with *O*-methoxyamine hydrochloride (15 mg/mL) in pyridine, and silylation with N,O-bis(trimethylsilyl)trifluoroacetamide in 1% trimethylchlorosilane. Finally, urine samples for CE-MS analysis were prepared by incubating 1 volume of urine with 4 volumes of 0.125 M formic acid. Quality control (QC) samples were prepared by pooling equal volumes of each sample and were injected every 6 samples injections and at the beginning/end of each analysis [13].

Fingerprinting of plasma with LC-QTOF/MS. A UHPLC system (Agilent 1290 Infinity LC System), equipped with a degasser, two binary pumps, and a thermostated autosampler coupled with Q-TOF LC/MS (6550 iFunnel) system (Agilent), was used in the ESI+ and ESI- mode to increase the number of detected metabolite ions as we previously described [10]. Briefly, 0.5 μL

of extracted plasma samples were injected into a thermostated (60ºC) RP Zorbax Extend C_{18} column (2.1 × 50 mm, 1.8 µm; Agilent Technologies). The flow rate was 0.6 mL/min with solvent A (water with 0.1% formic acid), and solvent B (acetonitrile with 0.1% formic acid). The chromatographic gradient started at 5% phase B during the first minute, followed by and increase of phase B to 80% (1-7 min) and 100% (7-11.5 min); the system was re-equilibrated by reverting the gradient to 5% phase B (12-15 min). The system was operated in full scan mode from 50-1000 m/z for positive and 50-1100 *m*/z for negative mode. Capillary voltage was set to 3 kV for positive and negative ionization modes; the drying gas flow rate was 12 L/min at 250 ºC and gas nebulizer at 52 psi; fragmentor voltage was 175V for positive and 250V for negative ionization mode; skimmer and octopole radio frequency voltage (OCT RF Vpp) were set to 65V and 750V, respectively. Data were collected in the centroid mode at a scan rate of 1.0 spectrum per second. Accurate mass measurements were obtained by means of an automated Calibrant Delivery System (CDS), using a Dual Agilent Jet Stream Electrospray Ionization (Dual AJS ESI) source that continuously introduces a calibrant solution with reference masses at m/z 121.0509 ($C_5H_4N_4$) and m/z 922.0098 ($C_{18}H_{18}O_6N_3P_3F_{24}$) in positive ionization mode or m/z 112.9856 8 ($C_2O_2F_3(NH_4)$) and 1033.9881 ($C_{18}H_{18}O_6N_3P_3F_{24}$) in negative ionization mode. Samples were analyzed in separate runs (positive and negative ionization mode), in a randomized order.

Fingerprinting of plasma with GC-Q-MS. A GC system (Agilent Technologies 7890A), equipped with an autosampler (Agilent 7693) and interfaced to an inert mass spectrometer with triple-Axis detector (5975C, Agilent), was used for fingerprinting as we have previously described [11, 14]. Briefly, 2 µL of the derivatized sample were injected in a GC-Column DB5-

MS (30 m length, 0.25 mm, 0.25 µm film 95% dimethyl/ 5% diphenylpolysiloxane) couple to a pre-column (10 m J&W integrated with Agilent 122-5532G). The injector port was held at 250 ºC, and the helium carrier gas flow rate was set at 1.0 mL/min. The split ratio was 1:10. The temperature gradient was programmed as follows: the initial oven temperature was set to 60 ºC (held for 1 min), increased to 325 ºC at a rate of 10 ºC/min; the system was allowed to cool down for 10 min before the next injection. The detector transfer line, the filament source and the quadrupole temperature were set to 280 ºC, 230 ºC and 150 ºC, respectively. MS detection was performed in electron impact (EI) mode at -70 eV. The mass spectrometer was operated in scan mode over a mass range of 50-600 m/z at a rate of 2.7 scan/s.

Fingerprinting of urine with CE-TOF/MS . An Agilent 7100 (CE) system, coupled to a TOF Mass Spectrometer (6224 Agilent), was used for samples analysis as published previously [12]. In brief, a fused-silica capillary (Agilent Technologies; total length, 96 cm; i.d., 50 µm) was pre-conditioned with 1M NaOH for 30 min, followed by MilliQ® water for 30 min and background electrolyte - BGE (0.8 M formic acid in 10% methanol) for 30 min. Before each analysis, the capillary was flushed for 5 min (950 mbar pressure) with BGE. The MS was operated in positive polarity, with a full scan from 80 to 1000 m/z at a rate of 1.4 scan/s. Drying gas was set to 10 L/min, nebulizer to 10 psi, voltage to 3.5 kV, fragmentor to 100V, gas temperature to 200 ºC and skimmer to 65V. The sheath liquid composition was methanol/water (1/1, v/v), containing 1.0 mmol/L formic acid with two references masses (121.0509 – purine ($C_5H_4N_4$) and 922.0098 – HP-921 ($C_{18}H_{18}O_6N_3P_3F_{24}$)), which allows for correction and provides more accurate mass determination. Flow rate was 0.6 mL/min and split was set to 1/100. Samples were injected at 50 mbar for 17 s. After each injection, along with the samples, BGE was co-injected for 10 s at 100

mbar pressure to improve repeatability. Separations were performed at a pressure of 25 mbar and a voltage of +30 kV; current under these conditions was 25 µA.

Data acquisition and statistical analysis

To provide quality assurance of results, LC-MS, GC-MC, CE-MS data treatment was performed as described previously [15]. Briefly, LC-MS and CE-MS raw data were cleaned from background noises and unrelated ions by the Molecular Feature Extraction tool (MassHunter Qualitative Analysis Software; Agilent). GC-MS data were analysed using the Agilent ChemStation Software (G1701EA E.02.00.493, Agilent). AMDIS 2.69 software from NIST (U.S. National Institute of Standards and Technology) was used for mass spectral deconvolution to identify co-eluted compounds according to their retention indices and retention times. GC-MS and CE-MS data were normalized according to C18:0 methyl ester and creatinine intensity, respectively. Primary data treatment (filtering and alignment) was performed with MPP (Mass Profiler Professional) B.12.1 software (Agilent). Variation of compound responses in QC-samples was expressed as CV. Metabolites detected in <50% of all QC-samples and with a CV >30% were removed to asure repeatability.

Univariate statistical analysis assuming equal (*t*-test) or unequal variance (Welch's *t*-test) and hierarchial heat map clustering analysis were performed with MPP B.12.1 software. Benjamin Hochberg FDR was applied for *P* value correction. Multivariate (unsupervised and supervised) analysis was performed using SIMCA-P+ 12.0 (Umetrics, Umea, Sweden). Associations between variables were tested by Spearman correlation coefficients (r_s) using Prism 6.0 software. Assessment of the diagnostic performance of the metabolites was made using the receiver

operating characteristic (ROC) curves by plotting the sensitivity against the corresponding false-positive rate (100-specificity), with the Prism 6.0 software. A test with perfect discrimination power yields a ROC curve that passes through the upper left corner with an AUC of one (100% sensitivity and 100% specificity). Thus, the closer the ROC-area to one, the higher the discriminant power of the metabolite. To construct the ROC curves, GDM was defined according to WHO-1998 criteria, as glucose level ≥140 mg/dl (7.8 mmol/l) after 2-h 75-g OGTT. To establish potential cutoff values for each metabolite, we determined the optimal decision point from the ROC curve, assigning equal weights to the sensitivity and specificity of the test.. Then, best sensitivity, specificity and likelyhood ratio for the selected cut-off of each parameter were obtained.

Compound identification

Identification of compounds (LC-MS and CE-MS) that were significant in class separation was performed by searching accurate masses against online databases (METLIN, HMDB, KEGG, LIPIDMAPS), and confirmed by LC-MS/MS. For CE-MS, compound identification was confirmed by using available standards. Compound identification by GC-MS was performed with the target metabolite Fiehn GC/MS Metabolomics RTL library (G1676AA, Agilent), the CEMBIO-library and the NIST mass spectra library 2.0, using the ChemStation software and native PBM (Probability-Based Matching) algorithm (G1701EA E.02.00.493, Agilent).

Experiment validation

Models obtained by multivariate calculations were validated by a cross-validation tool [16], using the "leaving one third out" approach. Prediction of excluded samples was reiterated until all samples were predicted at least once.

RESULTS

Study participants

There was no difference in age, parity or blood pressure between the women in the different groups (Table 1). BMI before gestation (BMIo) was similar in control and GDM women, despite a significantly higher BMI in 2nd trimester (BMI-2t). As expected, women who were classified as GDM according to WHO-criteria, had significantly higher fasting glucose, HbA1c, triacylglycerides and cholesterol than controls; HDL and LDL-cholesterol, basal insulin, C-peptide and CRP levels did not differ. During the OGTT, glucose levels were significantly higher at one and 2 hours in the women classified as GDM. The AUC-G was higher in the GDM women than in controls; there were no significant differences in HOMA-IR and QUICKI.

Correlation analysis shows that there was no association between the body weight gain (BMI-2t minus BMIo) and various measures of glycemic control and insulin resistance. We observed that both, BMIo and BMI-2t, correlated with glycemic condition (r_s for correlation with BMI-2t were 0.368, 0.424, 0.355, 0.485 and −0.455 for basal glucose, AUC-G, insulin, HOMA-IR and QUICKI, respectively; P<0.05 for all correlations). Significant correlations were also observed for plasma triacylglycerides and basal or 2h-glucose, AUC-G, insulin, HOMA-IR and QUICKI (r_s=0.412; 0.446; 0.460; 0.386; 0.453 and −0.501, respectively, P<0.01 for all correlations). No correlations were found between cholesterol (total, LDL, HDL) and basal or 2h-glucose, the

AUC-G, HOMA-IR and QUICKI indices (data not shown).

Metabolic fingerprinting

Metabolic fingerprinting allowed for the simultaneous detection of 114,431 potential compounds in plasma (LC: 114,347; GC: 84) and 7,428 in urine (CE). Data were filtered by choosing only those present in 100% (LC-MS/GC-MS) or 85% (CE-MS) of the samples in at least one of the groups. PCA analysis was used as an unsupervised method to get an overview and to detect trends within these data (626 in ESI+, 487 in ESI-; 48 in GC-MS; 127 in CE-MS). For LC-MS data, a clear separation can be observed between GDM and control groups, indicating metabolic changes inherent to GDM (Fig. 1*A*-*B*).

Supervised Partial Least Squares Discriminant Analysis (PLS-DA) and Orthogonal PLS Discriminant Analysis (OPLS-DA) were used for modeling differences between the groups. Figure 1*C*-*F* highlights the quality of the models, allowing for a clear separation of samples. To estimate the predictive power of the analysis, a cross-validation of PLS-DA models was performed. In the models obtained with data from LC-MS, 94% (ESI+) and 100% (ESI-) of all excluded samples were classified correctly; in data from GC-MS and CE-MS, 79% and 85%, respectively, of excluded samples were classified correctly.

Based on the compounds identified by LC-MS, we generated a metabolite heat map that revealed considerable differences between control and diabetic women (Fig. 2). Based on these findings, individual metabolites were compared, yielding statistical differences between control and GDM women in 571 metabolites in plasma (558 by LC-MS; 13 by GC-MS) and in 72 in urine (CE-

MS). To ensure valid measurements, metabolites with very high analytical variance (determined as CV in QC) were excluded from further analysis. Finally, we identified 142 compounds in plasma that were statistically different between the groups, including 83 glycerophospholipids (51 lyso- and 32 phosphoglycerides), 9 sphingophospholipids (6 sphingomyelins, 2 sphingoethanolamines, sphingosine phosphate); 25 fatty acids or derivatives (3 fatty acids, 20 modified fatty acids, 1 eicosanoid, 1 ketone body); carnitine and 5 acylcarnitines; 7 amino acids or modified aminoacids; 4 bile acid and derivatives; pyruvic and fumaric acid; glycerol; 1 vitamin; creatinine; 2-hydroxybutyrate, and 2 other compounds. In urine we identified 6 metabolites, including 5 aminoacids or derivatives, and carnitine. The most pronounced GDM-specific changes corresponded to lysophosphoglycerides, being the most abundant compounds lysophosphatidylcholines (LPC) with 16:0, 18:0, 18:1, 18:2, 18:3, 20:3, 20:4 and 20:5 acyl chains, followed by lysophosphatidylethanolamines (LPE) with 16:0, 18:0, 18:2, 20:0, 20:1, 20:2, 22:4 and 22:6 chains.

Table 2 shows metabolites that exhibited the highest significant differences between case and control groups. A complete list of metabolites identified by LC-MS that differed between experimental groups is available as supplementary material (Table 1S). Among the numerous glycerophospholipids that were determined, LPE(20:1), LPE(20:2), LPE(22:4), LPC(20:5), LPC(18:2), LPC(18:1), LPI(20:4), LPS(20:0), lysophosdatidic acid LPA(18:2), lipoxin C4, and the taurine-conjugates bile acids, trihydroxy-cholestanoyl taurine and taurolythocholic acid glucuronide showed a pronounced decrease with gestational diabetes, followed by other glycerophospholipids-species with poly-unsaturated fatty acids (PUFAs) as acyl moiety, glycerophosphocoline, long-chain PUFA (LC-PUFA) derivatives, such as araquidonate or docosahexaenoic acid methyl esters, conjugates bile acids, glycerophospholipids,

sphingophospholipids and acylcarnitines. Some metabolites showed an increase in the GDM group as compared to controls, including PE(38:6), PE(36:5), PC(38:1), PC(40:3), acetyl-carnitine, linoleic acid, glycerol, 3-hydroxybutyrate, 2-hydroxybutyrate, and fumaric acid (Table 2). In urine, we found a significant decrease of carnitine in GDM pregnant women, whereas hystidine, glutamine, phenylalanine, tryptophan and cystine were augmented in GDM.

We further compared the fatty acid chain of the lysoglycerophospholipids affected by GDM, and found not only a decrease in the total amount of lysoglycerophospholipids, but also a 1.7 fold increase of the ratio of saturated *versus* unsaturated fatty acids in GDM women as compared to controls (Fig. 3).

We performed a correlation analysis between all metabolites and diabetes outcome measures (fasting glucose, OGTT dynamics, HbA1c, HOMA-IR and QUICKI indices). Hundred and thirty-five metabolites correlated with the 2h-glucose (92 with $P<0.001$). Most metabolites correlated also with AUC-G, or HbA1c, but not with HOMA-IR or QUICKI. For simplicity, only those compounds that exhibited the highest Spearman coefficients (>+/-0.65) with 2-h glucose are shown (Table 3); correlations with fasting glucose, AUC-G, HbA1c and HOMA-IR are also included. Among metabolites that correlated with 2h-glucose, approximately 40% were lysoglycerophospholipids with a LC-PUFA moiety. The strongest associations were observed between 2h-glucose and arachidonic acid methylester (r_s=-0.7984), LPS (21:0) (r_s=0.7971), LPE(20:1) (r_s=-0.7934), trihydroxy-cholanoyl taurine (r_s=-0.7893), LPE(20:2) (r_s=-0,7812), LPC(18:2) (r_s=-0,7713), LPC(20:4) (r_s=-0,7684), LPC(18:1) (r_s=-0.7658), LPI(18:2) (r_s=-0.7649), LPS (20:0) (r_s=-0.7633); LPI(20:4) (r_s=-0.7576) and LPC(20:5) (r_s=-0.7531). Other lysoglycerophospholipids and glycerophospholipids with PUFAs in their lipid moiety had also significant strengths of association. Linoleic acid and dodecamide showed positive correlation

with 2h-glucose (P<0.05), whereas cerebronic acid and other fatty acid derivatives showed a negative correlation with the various measures of the glycemic state.

Other metabolites that were altered in GDM are acylcarnitines. Acetylcarnitine was increased by 30% in the GDM women (P=0.005) as compared to nondiabetic women (P=0.005), whereas long-chain acylcarnitines were reduced by approximately 30% (P<0.01) in the GDM women. Interestingly, in GDM women carnitine was also reduced by 30% in plasma (P=0.0001) and by 55% in urine (P=0.02). Correlation analyses revealed that plasma acetylcarnitine significantly correlated with 2h-glucose and AUC-G, whereas carnitine and LC-AC showed an inverse correlation with diabetes outcome measures; the highest correlation was found for steaorylcarnitine (-0.556, P=0.0002; −0.574, P=0.0001; −0.504, P=0.0009, for correlation with 2h-glucose, AUC-G and HbA1c, respectively). The ratio of long-chain acylcarnitines/carnitine was similar between control and diabetic women (0.38), whereas the acetyl-carnitine/carnitine ratio was significantly augmented in GDM (0.31 and 0.56 in control and GDM, respectively).

Finally, we performed a ROC analysis with metabolites that showed the best correlation with diabetes outcome. Only metabolites with a ROC area >0.94 are shown in Table 4. The analysis revealed a high discriminant power for 25 lysoglycerophospholipids, (21 contain a PUFA-chain), arachidonic (20:4) and docosahexaenoic (22:6) acid methylesters, and taurine-conjugated bile acids. Lipoxin was another lipid that exhibited a high discriminant power and also correlated with diabetic outcome.

DISCUSSION

Despite several recommendations, there is no consensus approach to GDM diagnosis [17]. Thus, the availability of metabolites (or metabolic patterns) that predict GDM would be a major advance. Here, we performed a multiplatform metabolomic analysis of pregnant women at the 2nd trimester in order to gain novel insights into the metabolic routes that are specifically altered in GDM and to identify potential biomarkers related to the glucose intolerance of the mother.

Metabolomic research in pregnancy has focused mainly on preeclampsia and, to our knowledge, only a few studies have analyzed potential urine biomarkers for GDM [18]. Here, we confirm results of a study on a large multiethnic population, reporting that changes in the urinary excretion profile during and after pregnancy do not yield reliable biomarkers for GDM [19]. In fact, the only alteration we detected in urine samples from GDM women was an increase in the excretion of some aminoacids that did not correlate with glycemic control of the women.

On the contrary, individual plasma metabolite fingerprints allowed for a clear discrimination of women with normal glucose tolerance and those with GDM. Identification of these metabolites revealed alterations of various metabolic pathways (for details see Fig. 4). Furthermore, we identified a set of metabolites, the variability of which correlated well with glycemic control and, thus, may provide insights into the metabolic disease etiology.

PHOSPHOLIPIDS and BILE ACIDS

Alterations of the levels and composition of plasma lysophospholipids were the most prominent changes that correlated well with the glycemic state of pregnant women. In particular, LPE(20:1) and (20:2) were affected by GDM and showed the highest discriminant power in the ROC analysis. Data about LPE as bioactive metabolites are scarce as compared to other phospholipids,

342 although its anti-inflammatory actions has been demonstrated in a mouse model of inflammation
343 [20]. In support of a role for LPE as a biomarker for GDM, a non-targeted metabolomic study
344 showed that LPE(16:1) allowed for the classification of subjects as insulin sensitive or insulin
345 resistant [21].

346 We also detected a decrease of various LPIs, in particular those with LC-PUFA(18:2, 20:4,
347 22:6), and of LPC, PC and glycerophosphocholine. We identified LPC(18:2) as one of the
348 metabolites that correlated best with the glycemic control of pregnant women and showed a high
349 discriminative power. Others have reported a decrease in various LPC, PC and
350 glycerophosphocoline in type 2-diabetes [22, 23] and, in various prospective population-based
351 cohort studies, low levels of LPC(18:2) were shown to be predictive for dysglycemia and type 2-
352 diabetes [5, 6]. Interestingly, LPCs, such as LPC(18:2), have been found to induce glucose-
353 induced insulin secretion from pancreatic β-cells, [5, 24, 25]. Furthermore, LPCs and LPSs were
354 found to improve glycemia in both normal and type 1 and 2 diabetic mice through an enhanced
355 glucose uptake [26, 27]. Thus, the observed decrease of lysoglycerophospholipids in GDM may
356 be associated with glucose intolerance through altered glucose metabolism and β-cell
357 dysfunction.

358 The observation that GDM was accompanied by a decrease in almost all species of
359 lysoglycerophospholipids, points to an alteration of a common enzymatic activity. Interestingly,
360 patients with IGT and type 2-diabetes were reported to have lower $cPLA_2$ (cytosolic calcium-
361 dependent phospholipase-A2 isoform) transcription levels [6]. Since PUFAs are typically
362 released from the sn-2 position of phospholipids, reduced cPLA2 activity could account for the
363 decreased concentration of arachidonic acid [6] or other LC-PUFAs associated to type 2-diabetes

[22].

Glycerophospholipids with shorter chain length and saturated fatty acid residues may trigger development of type 2-diabetes, whereas those containing LC-PUFAs may offer protection [23, 28] and attenuate inflammation induced by saturated acyl LPCs [29, 30], suggesting a role of lysoglycerophospholipids with LC-PUFAs as anti-inflammatory molecules. Interestingly, we found that the ratio of saturated/unsaturated acyl chains in LPCs, LPEs and LPIs was increased in GDM, indicating that lysoglycerophospholipids acyl moieties are determinant in their effect on glucose/lipid metabolism. These results, together with the decrease of lipoxin C4 levels in GDM, suggest that an unbalanced proportion of pro-inflammatory *versus* anti-inflammatory molecules is characteristic for GDM development. Interestingly, n-6 PUFA-derived lipoxins are potent anti-inflammatory compounds in various models of inflammation and, very recently, it has been proposed that they may act as endogenous anti-diabetic molecules [31].

In parallel with the decrease in lysoglycerophospholipids, we observed a decrease of plasmalogens in the GDM group. Various studies report a negative association of glycerophosphocholine-plasmalogens with obesity and insulin resistance [23, 32, 33]. As plasmalogens may act as serum antioxidants to prevent lipoprotein oxidation [33, 34], the decrease that we observed may suggest that low-grade lipid peroxidation occurs already at the beginning of GDM. In fact, in a previous study from our group [35], we found that, in the second trimester of gestation, non-obese women with GDM have already higher plasma concentrations of lipid and protein oxidation products than the control group.

We also observed a reduction in various sphingomyelins, ceramide-ethanolamines, and sphingosine 1-phosphate, although no significant differences were found in ceramides between

386 control and GDM pregnant women. Sphingolipid metabolism is altered in diabetic conditions
387 but, to date, most studies focused on ceramides [36] and only few examined the involvement of
388 sphingomyelins, obtaining contradictory results. Some studies found a decrease of some
389 sphingomyelins in diabetic patients [22, 23], whereas another study showed an increase [37].
390 Interestingly, whereas in the former studies, HbA1c was lower than 6.5%, the latter reported that
391 HbA1c was 8.3%. In this context, we found that GDM pregnant women at this stage of gestation
392 had a good glycemic control (HbA1c <5.5%). Since glucose activates sphingosine kinase,
393 favouring the synthesis of sphingosine 1-phosphate [38], we propose that sphingolipid variations
394 in diabetes are dependent of the metabolic control. Additionally, similar to other complex lipids,
395 the effects of sphingolipids may differ dependent on the acyl moiety. In support of this, type 1-
396 diabetes has been associated with a decrease in nervonic acid (24:1), and sphingomyelins-and
397 ceramides containing nervonic acid, whereas those with 20:0 and 24:0 acyl chains are increased
398 [39]. Interestingly, we found a decrease in hydroxy-nervonic acid in GDM, and it has been
399 reported that nervonic acid may have a preventive effect on human metabolic disorders [40]. As
400 detailed in Fig. 4, the observed decrease in sphingomyelins may be related to the partitioning of
401 palmitate to triacylglycerides in a competitive manner [41], favouring the hypertriglyceridemia
402 observed in GDM.

403 Taurine-conjugated bile acids also exhibited a strong inverse association with the glycemic state
404 and a high discriminating power between control and GDM pregnant women. Novel functions of
405 bile acid as metabolic integrators of energy homeostasis influencing glucose and lipid
406 metabolism have been described, including lowering triacylglycerides, inhibiting
407 gluconeogenesis, and improving insulin sensitivity [42]. In a metabolomic approach performed
408 in the KORA F3 cohort study, it was reported that cholate, a primary bile acid, was detected

more frequently in control subjects than in diabetics, while the opposite was found for deoxycholate, a secondary bile acid [22]. Accordingly, it has been suggested that the bile acid profile is altered in diabetes [43]. Whether the decrease in taurine-conjugated bile acids and/or the altered bile acid pool composition reflect on a metabolic change that could be involved in other GDM metabolic alterations, such as hypertriglyceridemia, or if it is solely discriminating between glucose intolerance under fasting conditions, needs to be examinated.

Other metabolites altered in GDM

We found that acetyl-carnititine, the main acylcarnitine ester, was increased in GDM, whereas carnitine and long-chain acyl-carnitines were decreased. This increase in acetyl-carnitine in GDM seems to be a common metabolic event of glucose homeostasis alterations, including IGT [6] and diabetes [44]. In fact, increased expression of carnitine acetyl-CoA transferase, the enzyme responsible for acetyl-carnitine synthesis, in blood cells has been reported for IGT and type 2-diabetes [6].

An altered fatty acid oxidation has been associated with insulin resistance and diabetes [45]. Interestingly, the early stages of diet-induced insulin resistance, when glucose intolerance but not insulin resistance is present, are characterized by increasing muscle fatty acid oxidation [46]. Furthermore, in different metabolomic studies it was found that medium-chain acylcarnitines decrease with impairing glucose tolerance [21]. The observed correlation of acetyl-carnitine and glucose intolerance tempts us to suggest that, at the beginning of gestation, an increased muscle fatty acid oxidation leads to a decrease in long-chain acylcarnitines, together with a concomitant increase of acetyl-CoA (Fig. 4). In fact, we observed a decrease in carnitine in the GDM group

that seems to be caused by the trapping effect of acetyl-CoA. This is supported by the observation that the ratio of long-chain acylcarnitines/carnitine did not differ between control and diabetic women, whereas the ratio acetyl-carnitine/carnitine was significantly augmented in the second group. Furthermore, the observed decrease in carnitine is considered a hallmark of glucose intolerance and insulin resistance [47].

We also found that glycine and pyruvate were significantly reduced in GDM. Recent metabolomics studies found a decrease of glycine in patients with IGT, type 2-diabetes, obesity, and impaired insulin sensitivity [21, 48], and in prospective studies, decreased glycine has also been proposed as an independent predictor of type 2-diabetes [23] and IGT [6]. Reduced glycine in GDM, may reflect on enhanced gluconeogenesis, glutathione synthesis [49] or both (detailed in Fig. 4). The role of glycine as an indicator of increased gluconeogenesis during fasting in the GDM group is further support by the fact that pyruvate is also significantly lower in GDM. It should be considered that, in fasting conditions, pyruvate is used preferentially for gluconeogenesis rather than for oxidation upon conversion to acetyl-CoA. Under these circumstances, fatty acids turn into the predominant susbtrate for energy production. A switch to fatty acid oxidation is further supported by increased levels of 3-hydroxybutyrate in GDM women under fasting conditions (this study), similar to what has been observed previously in the 2nd trimester of gestation in GDM [50].

Finally, we observed that plasma 2-hydroxybutyrate levels, an organic acid derived from 2-ketobutyrate in a reaction catalyzed by lactate dehydrogenase, were higher in GDM than in controls. 2-hydroxybutyrate is also elevated in human and animal models of type 2-diabetes [51] and has been proposed as an independent and early predictor of glucose intolerance in humans

[5, 21]. Accumulation of 2-hydroxybutyrate may occur *in vivo* when the formation of 2-ketobutyrate exceeds the rate of its catabolism. As detailed in Fig. 4, our interpretation that a redox imbalance may contribute to elevated 2-hydroxybutyrate is consistent with our finding that fatty acid oxidation is increased in GDM.

Concluding remarks

To our knowledge, this study represents the first multi-platform, non-targeted metabolome-wide analyses in plasma and urine of GDM. We show that, in the 2nd trimester of gestation, metabolite fingerprints in plasma reveal metabolic imbalances that are specific for human GDM. Some of the observed alterations have been previously associated with impaired glucose homeostasis. Nonetheless, we were able to identify specific metabolic patterns that are indicative of low-grade inflammation and altered redox-balance, which may reflect on the specific pathophysiological context of GDM. As this is a pilot study, future projects at later stages of gestation will allow us to validate the identified discriminant biomarkers as tools to predict the onset of diabetic complications both during pregnancy and after delivery.

Acknowledgments

The authors gratefully acknowledge the financial support from Spanish Ministry of Economy and Competitiveness (MINECO- CTQ2011-23562 and SAF2010-19603) and Community of Madrid (S2010/BMD-2423). D.D. acknowledges her postdoc contract with Universidad San Pablo-CEU. No potential conflicts of interest that are relevant to this article were reported. The authors thank all the study participants.

D.D. designed the study, performed experiments, analysed data, interpreted results and contributed to edition of the manuscript; M.Z. and G.K. contributed with the collection of samples, biochemical analysis and data acquisition; W.Z. contributed to biochemical analyis; M.S. and K.B-M. provided clinical data and expertise in clinical interpretation; M.V. and A.G. performed research and contributed to data analysis; C.B. is the guarantor of this work, contributed to the supervision of experiments and data interpretation; MP.R performed data analysis, coordinated data interpretation and wrote the manuscript. All authors reviewed and accepted the manuscript.

Part of this study was presented at the 49th Annual EASD Meeting (September 23-27, 2013) and at the 9th International Conference of the Metabolomics Society (July 1-4, 2013).

DISCLOSURES

No conflicts of interest, financial or otherwise, are declared by the authors.

488 REFERENCES

489

490 [1] Association AD. Diagnosis and classification of diabetes mellitus. Diabetes Care. 2009;32
491 Suppl 1:S62-7.
492 [2] International Association of D, Pregnancy Study Groups Consensus P, Metzger BE, Gabbe
493 SG, Persson B, Buchanan TA, et al. International association of diabetes and pregnancy study
494 groups recommendations on the diagnosis and classification of hyperglycemia in pregnancy.
495 Diabetes Care. 2010;33:676-82.
496 [3] Lowe LP, Metzger BE, Dyer AR, Lowe J, McCance DR, Lappin TR, et al. Hyperglycemia
497 and Adverse Pregnancy Outcome (HAPO) Study: associations of maternal A1C and glucose with
498 pregnancy outcomes. Diabetes Care. 2012;35:574-80.
499 [4] Bellamy L, Casas JP, Hingorani AD, Williams D. Type 2 diabetes mellitus after gestational
500 diabetes: a systematic review and meta-analysis. Lancet. 2009;373:1773-9.
501 [5] Ferrannini E, Natali A, Camastra S, Nannipieri M, Mari A, Adam KP, et al. Early metabolic
502 markers of the development of dysglycemia and type 2 diabetes and their physiological
503 significance. Diabetes. 2013;62:1730-7.
504 [6] Wang-Sattler R, Yu Z, Herder C, Messias AC, Floegel A, He Y, et al. Novel biomarkers for
505 pre-diabetes identified by metabolomics. Mol Syst Biol. 2012;8:615.
506 [7] Lowe WL, Jr., Bain JR. "Prediction is very hard, especially about the future": new
507 biomarkers for type 2 diabetes? Diabetes. 2013;62:1384-5.
508 [8] Matthews DR, Hosker JP, Rudenski AS, Naylor BA, Treacher DF, Turner RC. Homeostasis
509 model assessment: insulin resistance and beta-cell function from fasting plasma glucose and
510 insulin concentrations in man. Diabetologia. 1985;28:412-9.
511 [9] Katz A, Nambi SS, Mather K, Baron AD, Follmann DA, Sullivan G, et al. Quantitative
512 insulin sensitivity check index: a simple, accurate method for assessing insulin sensitivity in
513 humans. J Clin Endocrinol Metab. 2000;85:2402-10.
514 [10] Ciborowski M, Javier Ruperez F, Martinez-Alcazar MP, Angulo S, Radziwon P, Olszanski
515 R, et al. Metabolomic approach with LC-MS reveals significant effect of pressure on diver's
516 plasma. J Proteome Res. 2010;9:4131-7.
517 [11] Vallejo M, Garcia A, Tunon J, Garcia-Martinez D, Angulo S, Martin-Ventura JL, et al.
518 Plasma fingerprinting with GC-MS in acute coronary syndrome. Anal Bioanal Chem.
519 2009;394:1517-24.
520 [12] Moraes EP, Ruperez FJ, Plaza M, Herrero M, Barbas C. Metabolomic assessment with CE-
521 MS of the nutraceutical effect of Cystoseira spp extracts in an animal model. Electrophoresis.
522 2011;32:2055-62.
523 [13] Gika HG, Macpherson E, Theodoridis GA, Wilson ID. Evaluation of the repeatability of
524 ultra-performance liquid chromatography-TOF-MS for global metabolic profiling of human
525 urine samples. J Chromatogr B Analyt Technol Biomed Life Sci. 2008;871:299-305.
526 [14] Garcia A, Barbas C. Gas chromatography-mass spectrometry (GC-MS)-based
527 metabolomics. Methods Mol Biol. 2011;708:191-204.
528 [15] Dunn WB, Broadhurst D, Begley P, Zelena E, Francis-McIntyre S, Anderson N, et al.
529 Procedures for large-scale metabolic profiling of serum and plasma using gas chromatography
530 and liquid chromatography coupled to mass spectrometry. Nat Protoc. 2011;6:1060-83.

[16] Westerhuis J, Hoefsloot HJ, Smit S, Vis D, Smilde A, Velzen EJ, et al. Assessment of PLSDA cross validation. Metabolomics. 2008;4:81-9.
[17] Weinert LS. International Association of Diabetes and Pregnancy Study Groups recommendations on the diagnosis and classification of hyperglycemia in pregnancy: comment to the International Association of Diabetes and Pregnancy Study Groups Consensus Panel. Diabetes Care. 2010;33:e97; author reply e8.
[18] Fanos V, Atzori L, Makarenko K, Melis GB, Ferrazzi E. Metabolomics application in maternal-fetal medicine. Biomed Res Int. 2013;2013:720514.
[19] Sachse D, Sletner L, Morkrid K, Jenum AK, Birkeland KI, Rise F, et al. Metabolic changes in urine during and after pregnancy in a large, multiethnic population-based cohort study of gestational diabetes. PLoS One. 2012;7:e52399.
[20] Hung ND, Kim MR, Sok DE. 2-Polyunsaturated acyl lysophosphatidylethanolamine attenuates inflammatory response in zymosan A-induced peritonitis in mice. Lipids. 2011;46:893-906.
[21] Gall WE, Beebe K, Lawton KA, Adam KP, Mitchell MW, Nakhle PJ, et al. alpha-hydroxybutyrate is an early biomarker of insulin resistance and glucose intolerance in a nondiabetic population. PLoS One. 2010;5:e10883.
[22] Suhre K, Meisinger C, Doring A, Altmaier E, Belcredi P, Gieger C, et al. Metabolic footprint of diabetes: a multiplatform metabolomics study in an epidemiological setting. PLoS One. 2010;5:e13953.
[23] Floegel A, Stefan N, Yu Z, Muhlenbruch K, Drogan D, Joost HG, et al. Identification of serum metabolites associated with risk of type 2 diabetes using a targeted metabolomic approach. Diabetes. 2013;62:639-48.
[24] Soga T, Ohishi T, Matsui T, Saito T, Matsumoto M, Takasaki J, et al. Lysophosphatidylcholine enhances glucose-dependent insulin secretion via an orphan G-protein-coupled receptor. Biochem Biophys Res Commun. 2005;326:744-51.
[25] Metz SA. Ether-linked lysophospholipids initiate insulin secretion. Lysophospholipids may mediate effects of phospholipase A2 activation on hormone release. Diabetes. 1986;35:808-17.
[26] Yea K, Kim J, Yoon JH, Kwon T, Kim JH, Lee BD, et al. Lysophosphatidylcholine activates adipocyte glucose uptake and lowers blood glucose levels in murine models of diabetes. J Biol Chem. 2009;284:33833-40.
[27] Yea K, Kim J, Lim S, Kwon T, Park HS, Park KS, et al. Lysophosphatidylserine regulates blood glucose by enhancing glucose transport in myotubes and adipocytes. Biochem Biophys Res Commun. 2009;378:783-8.
[28] Kroger J, Zietemann V, Enzenbach C, Weikert C, Jansen EH, Doring F, et al. Erythrocyte membrane phospholipid fatty acids, desaturase activity, and dietary fatty acids in relation to risk of type 2 diabetes in the European Prospective Investigation into Cancer and Nutrition (EPIC)-Potsdam Study. The American journal of clinical nutrition. 2011;93:127-42.
[29] Riederer M, Ojala PJ, Hrzenjak A, Graier WF, Malli R, Tritscher M, et al. Acyl chain-dependent effect of lysophosphatidylcholine on endothelial prostacyclin production. J Lipid Res. 2010;51:2957-66.
[30] Hung ND, Sok DE, Kim MR. Prevention of 1-palmitoyl lysophosphatidylcholine-induced inflammation by polyunsaturated acyl lysophosphatidylcholine. Inflamm Res. 2012;61:473-83.
[31] Das UN. Arachidonic acid and lipoxin A4 as possible endogenous anti-diabetic molecules. Prostaglandins Leukot Essent Fatty Acids. 2013;88:201-10.

[32] Pietilainen KH, Sysi-Aho M, Rissanen A, Seppanen-Laakso T, Yki-Jarvinen H, Kaprio J, et al. Acquired obesity is associated with changes in the serum lipidomic profile independent of genetic effects--a monozygotic twin study. PLoS One. 2007;2:e218.
[33] Wallner S, Schmitz G. Plasmalogens the neglected regulatory and scavenging lipid species. Chem Phys Lipids. 2011;164:573-89.
[34] Engelmann B. Plasmalogens: targets for oxidants and major lipophilic antioxidants. Biochem Soc Trans. 2004;32:147-50.
[35] Ramos Alvarez MP, Viana M, Alcalá Díaz-Mor M, Bolado VE, Pita Santibáñez J, Espino M, et al. Gestational diabetes and obesity: role of oxidative stress and inflammation. FEBS Lett. 2012;279
[36] Deevska GM, Nikolova-Karakashian MN. The twists and turns of sphingolipid pathway in glucose regulation. Biochimie. 2011;93:32-8.
[37] Zhu C, Liang QL, Hu P, Wang YM, Luo GA. Phospholipidomic identification of potential plasma biomarkers associated with type 2 diabetes mellitus and diabetic nephropathy. Talanta. 2011;85:1711-20.
[38] Wang L, Xing XP, Holmes A, Wadham C, Gamble JR, Vadas MA, et al. Activation of the sphingosine kinase-signaling pathway by high glucose mediates the proinflammatory phenotype of endothelial cells. Circ Res. 2005;97:891-9.
[39] Fox TE, Bewley MC, Unrath KA, Pedersen MM, Anderson RE, Jung DY, et al. Circulating sphingolipid biomarkers in models of type 1 diabetes. J Lipid Res. 2011;52:509-17.
[40] Oda E, Hatada K, Kimura J, Aizawa Y, Thanikachalam PV, Watanabe K. Relationships between serum unsaturated fatty acids and coronary risk factors: negative relations between nervonic acid and obesity-related risk factors. Int Heart J. 2005;46:975-85.
[41] Watson ML, Coghlan M, Hundal HS. Modulating serine palmitoyl transferase (SPT) expression and activity unveils a crucial role in lipid-induced insulin resistance in rat skeletal muscle cells. Biochem J. 2009;417:791-801.
[42] Lefebvre P, Cariou B, Lien F, Kuipers F, Staels B. Role of bile acids and bile acid receptors in metabolic regulation. Physiol Rev. 2009;89:147-91.
[43] Staels B, Kuipers F. Bile acid sequestrants and the treatment of type 2 diabetes mellitus. Drugs. 2007;67:1383-92.
[44] Adams SH, Hoppel CL, Lok KH, Zhao L, Wong SW, Minkler PE, et al. Plasma Acylcarnitine Profiles Suggest Incomplete Long-Chain Fatty Acid β-Oxidation and Altered Tricarboxylic Acid Cycle Activity in Type 2 Diabetic African-American Women. J Nutr. 2009;139:1073-81.
[45] Schooneman MG, Vaz FM, Houten SM, Soeters MR. Acylcarnitines: reflecting or inflicting insulin resistance? Diabetes. 2013;62:1-8.
[46] Trajcevski KE, O'Neill HM, Wang DC, Thomas MM, Al-Sajee D, Steinberg GR, et al. Enhanced lipid oxidation and maintenance of muscle insulin sensitivity despite glucose intolerance in a diet-induced obesity mouse model. PLoS One. 2013;8:e71747.
[47] Poorabbas A, Fallah F, Bagdadchi J, Mahdavi R, Aliasgarzadeh A, Asadi Y, et al. Determination of free L-carnitine levels in type II diabetic women with and without complications. Eur J Clin Nutr. 2007;61:892-5.
[48] Wurtz P, Makinen VP, Soininen P, Kangas AJ, Tukiainen T, Kettunen J, et al. Metabolic signatures of insulin resistance in 7,098 young adults. Diabetes. 2012;61:1372-80.

[49] Sekhar RV, McKay SV, Patel SG, Guthikonda AP, Reddy VT, Balasubramanyam A, et al. Glutathione synthesis is diminished in patients with uncontrolled diabetes and restored by dietary supplementation with cysteine and glycine. Diabetes Care. 2011;34:162-7.
[50] Montelongo A, Lasuncion MA, Pallardo LF, Herrera E. Longitudinal study of plasma lipoproteins and hormones during pregnancy in normal and diabetic women. Diabetes. 1992;41:1651-9.
[51] Salek RM, Maguire ML, Bentley E, Rubtsov DV, Hough T, Cheeseman M, et al. A metabolomic comparison of urinary changes in type 2 diabetes in mouse, rat, and human. Physiol Genomics. 2007;29:99-108.

Figure 1. Score plots of plasma (A-E) and urine (F) metabolic profiles obtained for control (□) and GDM women (○).

A-B. Unsupervised PCA analysis.

(A) LC-MS ESI+ (R^2=0.53, Q^2=0.48) (**B)** LC-MS ESI- (R^2=0.43, Q^2=0.34). The plots indicate that healthy controls can be clearly separated from most of GDM individuals.

C-F. Supervised OPLS/O2PLS-DA analysis.

C, D- OPLS/O2PLS-DA model (R^2= 0.97, Q^2=0.83 and R^2= 0.99, Q^2=0.9) built for the two groups (GDM women *versus* healthy controls) based on 626 LC-MS ESI+ (C) and 487 LC-MS ESI- (D) detected variables.

E, F- OPLS/O2PLS-DA model built for the two groups according to 48 GC-MS (R^2=0.75, Q^2=0.5) (E) and 127 CE-MS (R^2= 0.91, Q^2=0.69) (F) detected variables.

R^2= coefficient for variance explained; Q^2= coefficient for variance predicted.

Figure 2. Dendrogram and heat map of plasma metabolites.

Cluster analysis of LC-MS data was performed in order to identify patterns of metabolites that discriminate between control and GDM women. The heat map represents the signal intensities of 20 pregnant women with normal glucose tolerance (■), and 20 pregnant women that were diagnosed with GDM (■) according to the 2h-OGTT. Colors reflect on signal intensity; measured in plasma samples. The spectrum ranging from red to blue represents the range of high to low signal intensities, respectively, for each metabolite, identified by numbers as described below. Black color indicates missing values. The X-axis was divided into two sections by a white discontinuous line, representing 2h-glucose below or above the threshold value of >140 mg/dL (7,8 mM) for diagnosis of GDM. The Y-axis was divided into three sections, representing high, medium and low metabolite concentrations (the identification of all compounds is available as supplementary material). Two samples, classified as control (17C) and GDM (20D) according to the 2h-OGTT, are marked with arrows to highlight a different metabolic pattern of their corresponding group. Follow-up of these women throughout pregnancy revealed that, two weeks before delivery, the study participant 17C who was classified as control had HbA1c of 9%. The GDM woman 20D received dietary treatment and, during the rest of gestation, fasting glucose fell below 100 mg/dL (5.55 mM).

1-SM(34:1); **2**-Oleamide; **3**-LPC(16:0); **4**-SM(36:2); **5**-SM(34:2); **6**-LPC(18:2)sn-2; **7**-Linoleamide; **8**-Palimitic amide; **9**-LPA(16:0); **10**-Dodecanamide; **11**-LPI(16:1); **12**-LPI(16:0); **13**-PC(40:3); **14**-PC(38:1); **15**-PC(32:2); **16**-PE(36:3); **17**-LPC(18:1)sn-2; **18**-LPC(18:0)sn-2; **19**-PC(36:6); **20**-Docosenamide; **21**-PC(35:4); **22**-PC(O-38:6) or PC(P-38:5); **23**-LPE(20:1); **24**-LPE(20:0); **25**-LPE(18:0);

26-LPC(18:3)sn-2; **27**-LPE(20:2); **28**-Oleoyl Ethylamide; **29**-Octadecatrienal; **30**-PE(38:5); **31**-PC(40:9); **32**-PC(40:7); **33**-Octadecatrienol; **34**-PC(36:5); **35**-PC(40:8); **36**-PC(38:7); **37**-LPE(16:0); **38**-SM(36:3); **39**-PC(38:5); **40**-LPE(22:6); **41**-LPE(22:4); **42**-Asparylthreonine; **43**-Acetylglutamine; **44**-Phosphatidyl-myo-inositol; **45**-PC(36:4); **46**-LPE(20:4); **47**-PC(P-36:5); **48**-LPE(18:1); **49**-LPE(O-18:1) or LPE(P-18:0); **50**-LPI(18:2); **51**-LPC(22:5)sn-2; **52**-LPC(20:4)sn-2; **53**-LPC(17:0)sn-2; **54**-LPC(O-16:0)sn-1; **55**-Acetylcarnitine; **56**-PC(42:7); **57**-LPC (20:3)sn-1; **58**-LPI(20:4); **59**-LPS(20:0); **60**-LPC(20:5)sn-2; **61**-Lipoxin C4; **62**-LPE(18:2); **63**-LPC(16:1)sn-2; **64**-SM(32:2); **65**-Hexadecatrienol; **66**-Trioxocholenoic acid; **67**-PC(35:3); **68**-Carnitine; **69**-Taurolithocholic acid glucuronide; **70**-PC(19:1); **71**-PE(38:6); **72**-PE(36:5); **73**-Asparylhydrohyproline; **74**-Cerebronic acid; **75**-PS(26:0); **76**-PC(21:0 (COOH)); **77**-LPI(20:3); **78**-LPC(22:6)sn-2; **79**-LPC(22:4)sn-2; **80**-Oxo-nonadecanoic acid; **81**-LPS(20:2); **82**-Hydroxynervonic acid; **83**-LPE(19:0); **84**-LPA(18:2); **85**-LPE(18:3); **86**-LPE(22:1); **87**-LPC(O-18:1)sn-1 or LPC (P-18:O)sn-1; **88**-PC(27:0); **89**-LPC(19:1); **90**-Stearoylcarnitine; **91**-Linoleylcarnitine; **92**-PC(42:9); **93**-SM(33:2); **94**-Trihydroxy-cholestanoyl taurine; **95**-LPC(20:2)sn-2; **96**-Glycerophosphocholine; **97**-Arachidonic Acid Methylester; **98**-Docosahexaenoic Acid Methylester; **99**-PC(21:1); **100**-PC(42:8); **101**-Dihydroxytetranorvitamin D3; **102**-Pentadecadienal; **103**-PC(19:0); **104**-LPI(22:6); **105**-Anandamide (20:2, n-6); **106**-LPE(P-20:0); **107**- LPC(20:0)sn-2; **108**-LPC(17:1)sn-2; **109**-LPC(24:0)sn-2; **110**-LPC(O-18:0)sn-1; **111**-Dimethyl-undecadienone; **112**-Tetradecadienal; **113**-Tetramethyltridecadienal; **114**-Dodecadienal; **115**-Oxo-heneicosanoic acid; **116**-Sphingosine-phosphate; **117**-Palmitoylcarnitine; **118**-PA(28:0); **119**-PA(38:6); **120**-LPC(14:0)sn-2; **121**-Epoxy-dimethyl-cyclocholestan-ol; **122**-PE-Cer(34:1); **123**-LPE(P-16:0); **124**-LPC(20:1)sn-1; **125**-Palmitoyl Isopropylamide; **126**-LPC(15:0)sn-2; **127**-PE-Cer(33:1); **128**-Vaccenylcarnitine; **129**-PC(42:10); **130**-Hydroxy-oxo-cholanoic acid; **131**-Histidine.

Figure 3. Comparative description of the main lysoglycerophospholipids in control and GDM pregnant women at the second trimester of gestation.

(**A**) lysophosphatidylcholines (LPC); (**B**) lysophosphatidylethanolamines (LPE) and (**C**) lysophosphatidylinositols (LPI).

Data are given in percentage (%) and represent the area of the lysoglycerophospholipids with saturated, monounsaturated (MUFA) or polyunsaturated (PUFA) acyl chains relative to the total area.

Figure 4. Proposed model of metabolic alterations in the second trimester of GDM, with a special focus on lipid metabolism.

We hypothesized that, at beginning of pregnancy, GDM is characterized by an increased response to fasting. During this response, fatty acids (NEFA) turn into the major substrate for energy production, favouring oxidative stress and a mild inflammatory condition. In this scenario, an enhanced lipolysis (**1**) in adipose tissue (supported by increased glycerol and linoleic acid (C18:2)) favors liver and muscle NEFA availability. In both tissues, lipid overload drives an

intramitochondrial flux of acyl-CoA for NEFA oxidation, which results in decreased long-chain acylcarnitines (LC-AC) and accumulation of acetyl-CoA (**2**). This metabolite is converted into acetyl-carnitine (**3**), permitting its mitochondrial efflux that otherwise would inhibit *pyruvate dehydrogenase*. This situation causes depletion of carnitine and, consequently, decreased excretion of this metabolite into the circulation as well as increased levels of circulating acetyl-carnitine (**4**).

In humans, the liver accounts for most of the NEFA oxidation during fasting. In this condition, acetyl-CoA can be used for 3-hydroxybutyrate (3-HB) synthesis, contributing to the ketonemia observed in GDM women (**5**), or may activate *pyruvate carboxylase*, favoring gluconeogenesis (**6**). Thus, pyruvate and glycerol (**7**) are used preferentially for gluconeogenesis, favouring glucose intolerance (**8**). Reduced glycine in GDM may also reflect on enhanced gluconeogenesis, since glycine can be converted to glucose via pyruvate production or/and, to glutathione (GSH) (**9**).

Enhanced mitochondrial activity also increases the $NADH+H^+/NAD^+$ ratio and oxygen radical production (**2**). To cope with the resulting oxidative stress, glutathione biosynthesis is activated (**10**), which is supported by the observed decreased in glycine and glutamate and the concomitant increase of 2-hydroxybutyrate (2-HB). 2-ketobutyrate (2-KB) is produced through the conversion of cystathionine to cysteine for glutathione biosynthesis (**11**). Subsequently, 2-KB is reduced to 2-HB (**12**), which is favored by the observed increase of the $NADH/NAD^+$ ratio (**2**). Thus, 2–HB is associated with an increased demand for glutathione biosynthesis and disrupted mitochondrial energy metabolism.

The reduced *de novo* sphingolipid synthesis found in GDM, probably as a consequence of serine availability (**13**), favors the flux of palmitate (16:0) towards TG, leading to the hypertrigliceridemia observed in GDM women (1**4**). In this condition, enhanced TG biosynthesis may also cause that phosphatidic acid is not used for the synthesis of glycerophospholipids (PL) (**15**), favouring the observed decrease in lysophospholipids (LysoPL). The fact that cysteine metabolism is favoring glutathione biosynthesis may be associated with a decrease in SAM, a key molecule for the transformation of PC to PE in the liver.

Finally, *de novo* sphingolipid synthesis is reduced (**13**); probably ceramides are synthesized via sphingomyelin hydrolysis or through the salvage pathway from sphingosine 1-phosphate (S1P) (**16**), which would explain the observed decrease of these lipids. Decreased ethanolamine-plasmalogen (Et-Plasm) levels may be a consequence of their increased utilization as antioxidants (**17**) or of a decreased synthesis from S1P (**18**).

Other abbreviations: OAA: oxaloacetate; 2-KG: 2-ketoglutarate.

Arrows indicate whether the level of a given metabolite was increased (red) or decreased (blue) according to the metabolome analysis performed in the present study Discontinuous arrows represent a reduced utilization of the corresponding metabolic route.

739 **** gluconeogenesis*** takes place only in the liver.

*Graphical Abstract (for review)

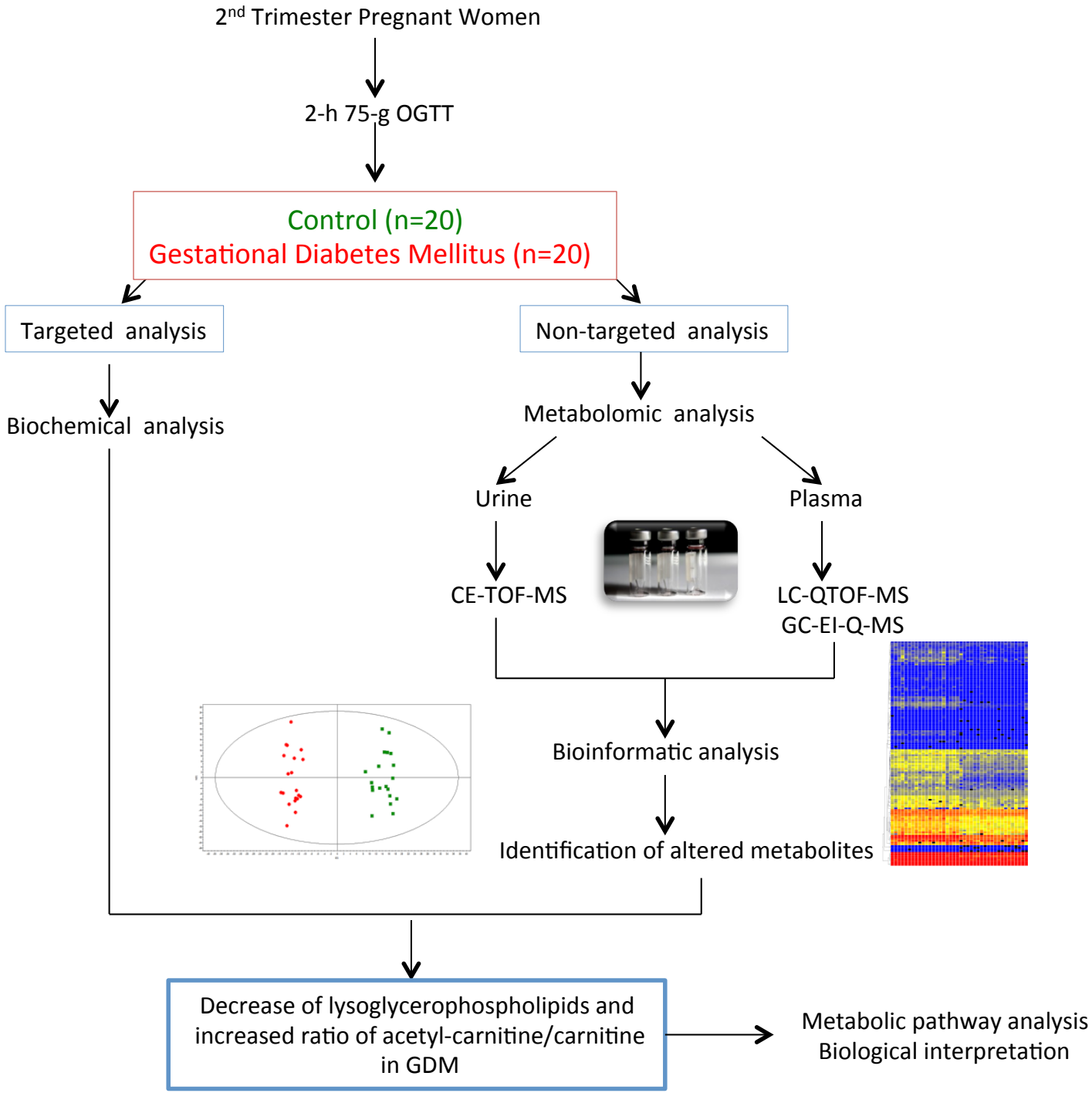

***Highlights (for review)**

- First multiplatform non-targeted metabolomic analysis of human gestational diabetes.
- Plasma fingerprints reveal disease-specific metabolic imbalances in diabetic women.
- Lysoglycerophospholipids reflect on glucose intolerance in gestational diabetes.

Table 1
Click here to download Table: Ramos at al Table 1.docx

Table 1. Anthropometric and metabolic characteristic of the women included in the study.

Parameter	Control group n=20	GDM group n=20	*P*-value
Age (years)	28.5 ± 2.7	28.1 ± 4.7	ns
Parity (number)	1.3 ± 0.6	1.4 ± 0.8	ns
Week of gestation	24.8 ± 1.3	25.5 ± 1.6	ns
Pre-pregnancy BMI (kg/m^2)	22.0 ± 2.7	24.6 ± 5.1	ns
Pregnancy BMI (kg/m^2)	23.8 ± 2.5	27.4 ± 5.5	0.01
Fasting glucose (mmol/L)	4.41 ± 0.29	5.10 ± 0.79	0.001
1-h glucose, OGTT (mmol/L)	6.64 ± 0.91	8.99 ± 1.87	<0.0001
2-h glucose, OGTT (mmol/L)	5.76 ± 0.91	8.97 ± 1.02	<0.0001
AUC-G	12680 ± 1316	17324 ± 2204	<0.0001
HbA1$_C$ (%) **(mmol/mol)**	4.78 ± 0.31 28.7 ± 3.4	5.23 ± 0.39 33.6 ± 4.3	0.0003
Insulin (pmol/L)	73.8 ± 22.0	78.5 ± 35.5	ns
C Peptide (pmol/L)	0.53 ± 0.16	0.58 ± 0.21	ns
HOMA-IR	2.43 ± 0.78	2.98 ± 1.44	ns
QUICKI	0.34 ± 0.02	0.33 ± 0.02	ns
Triacylglycerides (mmol/L)	1.58 ± 0.60	2.19 ± 0.64	0.004
Total cholesterol (mmol/L)	6.30 ± 0.95	6.94 ± 0.92	0.038
LDL-cholesterol (mmol/L)	3.51 ± 0.76	3.75 ± 0.91	ns
HDL-cholesterol (mmol/L)	2.13 ± 0.45	2.23 ± 0.42	ns
CRP (μg/ml)	3.94 ± 3.29	4.94 ± 3.94	ns
Systolic blood pressure (mmHg)	117.0 ± 7.2	117.0 ± 11.8	ns
Diastolic blood pressure (mmHg)	72.3 ± 9.6	71.6 ± 9.6	ns

Presented data are mean **±** SD. Statistical comparisons assuming equal (*t* test) or unequal variance (Welch's *t* test) were performed as appropriate. AUC-G: Area under the curve of glucose during the OGTT. Results were considered significant when $P<0.05$.

Table 2
Click here to download Table: Ramos at al Table 2.docx

Table 2. List of selected metabolites identified in plasma or urine by a multiplatform metabolomic analysis that exhibit the most significant changes with gestational diabetes.

Identified compound	*P* value	Change (%)	CV in QC (%)
LC-MS (Plasma)			
LPE(20:2)	6.66E-15	-66	7
LPE(20:1)	2.08E-14	-59	4
Trihydroxy-cholestanoyl taurine	9.70E-14	-53	5
LPA(18:2)	1.54E-13	-56	18
LPC(20:5) sn-2	8.27E-13	-73	14
LPI(20:4)	1.43E-12	-75	8
LPC(18:2) sn-2	1.72E-12	-66	15
PC(21:1)	1.72E-12	-77	23
LPC(18:1) sn-2	5.32E-12	-63	11
LPE(22:4)	5.66E-12	-59	6
LPS(20:0)	6.07E-12	-63	7
Lipoxin C4	8.26E-12	-39	10
LPC(22:5) sn-2	9.77E-12	-70	12
LPC(22:4) sn-2	1.67E-11	-69	16
LPI(18:2)	2.38E-11	-73	9
LPC(20:2) sn-2	2.60E-11	-67	15
LPC(20:4) sn-2	3.55E-11	-76	12
Taurolithocholic acid glucuronide	4.93E-11	-60	23
LPC(19:1)	1.90E-10	-54	11
Glycerophosphocholine	3.22E-10	-61	4
Docosahexaenoic acid Methylester	3.25E-10	-73	11
LPI(22:6)	4.66E-10	-70	26
Arachidonic acid Methylester	7.76E-10	-72	19
LPC(22:6) sn-2	1.02E-09	-55	9
LPI(20:3)	1.86E-09	-67	20
LPE(18:2)	4.61E-08	-51	5
LPE(20:4)	6.25E-08	-52	7

LPE(22:6)	6.40E-08	-44	4
GC-MS (Plasma)			
Creatinine	3.1E-5	-49	10
Pyruvic acid	5.0E-5	-54	
L-tryptophan	2.0E-3	-24	25
2-hydroxybutyric acid	3.3E-3	68	13
Glycine	6.2E-3	-39	15
L-glutamic acid	1.7E-2	-14	11
Lauric acid	1,9E-2	-24	8
Glycerol	3.4E-2	19	14
3-hydroxybutyric acid	5.0E-2	75	
Linoleic acid	5.0E-2	19	11
Fumaric acid	5.0E-2	15	
CE-MS (Urine)			
Carnitine	2.99E-02	-46	12
Histidine	3.20E-02	32	4
Glutamine	JK	36	15
Phenylalanine	JK	19	4
Tryptophan	JK	23	4
Cystine	JK	24	7

For LC-MS only those metabolites with *P* values $<1.10^{-7}$ are shown. The complete list of compounds is included as supplementary material. For GC-MS and CE-MS all compounds with $P < 0.05$ between GDM and controls are shown. % change represents the increase (+) or decrease (-) of the mean in the gestational diabetes group with respect to the control group, the sign indicates the direction of the change. CV in QC indicates the % of variation of the quality control that was included in the analysis. When necessary data were transformed by applying a log(base 2) in order to approximate a normal distribution. Univariate statistical analysis assuming equal (*t* test) or unequal variance (Welch's *t* test) were performed as appropriate. *P* value was corrected according FDR test and $P < 0.05$ was considered significant. Multivariate statistical analysis Jack-Knife (JK) confidence intervals estimative, 95% confidence level.

Table 3
Click here to download Table: Ramos at al Table 3.docx

Table 3. Correlation analysis.

Compound	0h glucose	2h Glucose	AUC-G	HBA_{1C}	HOMA
Arachidonic acid methylester	-0.4152**	-0.7984$^{###}$	-0.7331$^{###}$	-0.5228***	-0.1974
LPS(21:0)	-0.3342*	-0.7971$^{###}$	-0.6743$^{##}$	-0.5052***	-0.1353
LPE(20:1)	-0.3410*	-0.7934$^{###}$	-0.6720$^{##}$	-0.5076***	-0.1447
Trihydroxy-cholestanoyl taurine	-0.3374*	-0.7893$^{###}$	-0.6631$^{#}$	-0.4908**	-0.1519
LPE(20:2)	-0.3869*	-0.7812$^{###}$	-0.6799$^{##}$	-0.5394**	-0.0712
LPC(18:2)sn-2	-0.3984*	-0.7713$^{###}$	-0.6893$^{##}$	-0.5530**	-0.1790
LPC(20:4)sn-2	-0.3391*	-0.7684$^{###}$	-0.6691$^{##}$	-0.4808**	-0.2090
LPC(18:1)sn-2	-0.3183*	-0.7658$^{###}$	-0.6392$^{##}$	-0.4753**	-0.1664
LPI(18:2)	-0.3804*	-0.7649$^{###}$	-0.6577$^{##}$	-0.5348***	-0.1112
LPS(20:0)	-0.3909*	-0.7633$^{###}$	-0.7062$^{###}$	-0.5194***	-0.1006
LPI(20:4)	-0.3675*	-0.7576$^{###}$	-0.6762$^{##}$	-0.4601**	-0.0846
LPC(20:5)sn-2	-0.4028**	-0.7531$^{###}$	-0.6801$^{##}$	-0.5204***	-0.2019
Taurolithocholic acid glucuronide	-0.3344*	-0.7489$^{###}$	-0.6392$^{#}$	-0.4117**	-0,1121
LPE(22:4)	-0.3619*	-0.7472$^{###}$	-0.6936$^{##}$	-0.5183***	-0,0258
LPC(19:1)	-0.3856*	-0.7424$^{###}$	-0.6833$^{##}$	-0.4568**	-0.1568
LPE(18:2)	-0.3354*	-0.7420$^{###}$	-0.6329$^{#}$	-0.5196***	-0.1478
Glycerophosphocholine	-0.1958	-0.7419$^{###}$	-0.6717$^{##}$	-0.3537*	-0.2752
PC(21:1)	-0.3677*	-0.7416$^{###}$	-0.6801$^{##}$	-0.5042***	-0.1872
LPE(22:1)	-0.4061**	-0.7368$^{###}$	-0.7082$^{###}$	-0.4431**	-0.2346
LPI(22:6)	-0.4143*	-0.7279$^{###}$	-0.6426$^{##}$	-0.4641**	-0.0894
LPA(18:2)	-0.3502*	-0.7241$^{###}$	-0.6421$^{#}$	-0.4497**	-0.1840
LPI(16:1)	-0.4845**	-0.7206$^{##}$	-0.6073***	-0.4985**	-0.0478
Docosahexaenoic acid methylester	-0.3914*	-0.7186$^{###}$	-0.6787$^{##}$	-0.4716**	-0.2203
LPC(O-18:0)sn-1	-0.3112*	-0.7150$^{###}$	-0.6155$^{#}$	-0.4048**	-0.3264*
LPE(22:6)	-0.3774*	-0.7080$^{##}$	-0.6403$^{##}$	-0.4790**	-0.1102
Dihydroxy-cholestanoyl taurine	-0.2415	-0.7065$^{###}$	-0.6010$^{#}$	-0.3503*	-0.0955
LPC(22:5)sn-2	-0.3581*	-0.6956$^{##}$	-0.5983$^{#}$	-0.4273**	-0,1983
LPC(22:4)sn-2	-0.3917*	-0.6953$^{##}$	-0.6136$^{#}$	-0.4745**	-0.1547
LPC(20:2)	-0.3725*	-0.6952$^{##}$	-0.5867$^{#}$	-0.4072**	-0.2029
LPC(22:6)sn-2	-0.3288*	-0.6915$^{##}$	-0.5956***	-0.4266**	-0.1448
LPC(O-16:0)sn-1	-0.2589	-0.6899$^{##}$	-0.5984$^{#}$	-0.3703	-0.2656
LPC(20:1)sn-1	-0.3770*	-0.6896$^{##}$	-0.6290$^{#}$	-0.4484**	-0,3447*
PC(O-38:6) or PC(P-38:5)	-0.3214*	-0.6867$^{##}$	-0.5977***	-0.3761	-0.1471
Epoxy-dimethyl-cyclocholestanol	-0.2428	-0.6857$^{##}$	-0.6273$^{#}$	-0.3922*	-0.0507
LPE(O-18:1) or LPE(P-18:0)	-0.2607	-0.6843$^{##}$	-0.6250$^{#}$	-0.3637*	-0.1600
LPC(O-18:1) or LPC (P-18:O)	-0.3295*	-0.6823$^{##}$	-0.6303$^{#}$	-0.3168*	-0.3789*
LPI(20:3)	-0.5047**	-0.6811$^{##}$	-0.6662$^{##}$	-0.5162**	-0.2676
PE(36:3)	-0.3061	-0.6810$^{##}$	-0.6929$^{##}$	-0.2945	-0.3165*
LPE(P-16:0)	-0.1444	-0.6781$^{##}$	-0.5392***	-0.2141	-0.2523
LPE(20:0)	-0.3108	-0.6712$^{##}$	-0.6208$^{#}$	-0.4380**	-0.1533
LPE(15:1)	-0,2123	-0.6670$^{##}$	-0.6027$^{#}$	-0.3163*	-0.1365
Palmitoyl isopropylamine	-0.2839	-0.6634$^{##}$	-0.5471***	-0.3960*	-0.1194

Oleoyl ethylamine	-0.3307*	-0.6629##	-0.5277***	-0.4320**	-0.1164
PC(19:0)	-0.2964	-0.6592##	-0.6035***	-0.3338*	-0.2048
LPC(18:0)	-0.2370	-0.6582##	-0.5625***	-0.3575*	-0.2002
Lipoxin C4	-0.3367*	-0.6577##	-0.6010#	-0.4673**	-0.1615

Only metabolites with Spearman coefficients (r_s) higher than 0.65 for correlation with 2h-glucose are shown. * $P< 0.05$; ** $P< 0.01$; *** $P< 0.001$; # $P< 0.0001$; ## $P< 0.00001$; ### $P< 0.000001$. Correlations with P value < 0.0001 are color in gray.

Table 4
Click here to download Table: Ramos at al Table 4.docx

Table 4. ROC analysis.

Compound	AUC	*P* value	Sensitivity (%)	Specificity (%)	Likelihood Ratio
LPC(18:1)	0.988	<0.0001	100	95	19
LPC(18:2)	0.990	<0.0001	100	95	20
LPC(19:1)	0.960	<0.0001	90	95	18
LPC(20:1)	0.940	<0.0001	90	95	18
LPC(20:2)	0.980	<0.0001	95	95	19
LPC(20:4)	0.980	<0.0001	95	95	19
LPC(20:5)	0.988	<0.0001	100	95	20
LPC(22:4)	0.983	<0.0001	95	95	19
LPC(22:5)	0.990	<0.0001	90	95	18
LPC(22:6)	0.971	<0.0001	90	95	18
LPE(18:2)	0.965	<0.0001	80	95	16
LPE(20:0)	0,950	<0.0001	85	95	17
LPE(20:1)	0.995	<0.0001	100	95	20
LPE(20:2)	0.995	<0.0001	100	95	20
LPE(22:1)	0.945	<0.0001	95	95	19
LPE(22:4)	0.985	<0.0001	100	95	20
LPE(22:6)	0.958	<0.0001	75	95	15
LPS(20:0)	0.995	<0.0001	100	95	20
LPS(21:0)	0.995	<0.0001	100	95	20
LPS(22:0)	0.960	<0.0001	90	95	18
LPI(18:2)	0.990	<0.0001	100	95	20
LPI(20:3)	0.969	<0.0001	75	95	15
LPI(20:4)	0.980	<0.0001	100	95	19
LPI(22:6)	0,973	<0.0001	95	95	19
LPA(18:2)	0.990	<0.0001	100	95	20
PC(21:1)	0.988	<0.0001	100	95	20
Docosahexaenoic acid methylester	0.975	<0.0001	95	95	19
Araquidonate methylester	0.968	<0.0001	95	95	19
Glycerophosphocholine	0.959	<0.0001	94	95	19
Lipoxin C4	0.943	<0.0001	90	95	18
Trihydroxy-cholestanoyl taurine	0.995	<0.0001	100	95	20
Taurolithocholic glucuronide	0.990	<0.0001	95	95	19

Receiver-operating characteristic (ROC) curves were prepared by plotting the sensitivity against the corresponding false-positive rate (100-specificity). Table shows the area under the curve (AUC), and the best sensitivity, specificity and likelyhood ratio for a selected cut-off of each parameter.

Figure 1

Figure 1

Click here to download Figure: Figure 1 new.pdf

Unsupervised PCA analysis

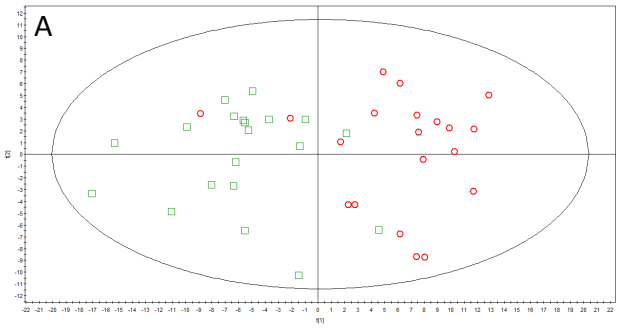

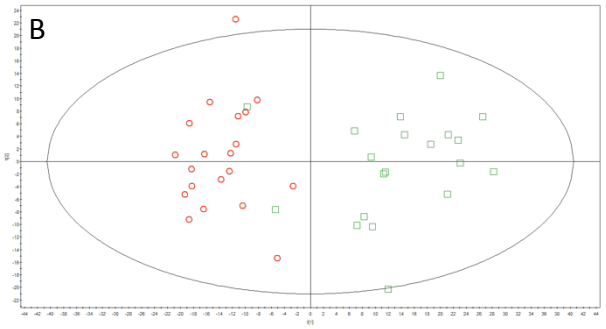

Supervised OPLS/O2PLS-DA analysis

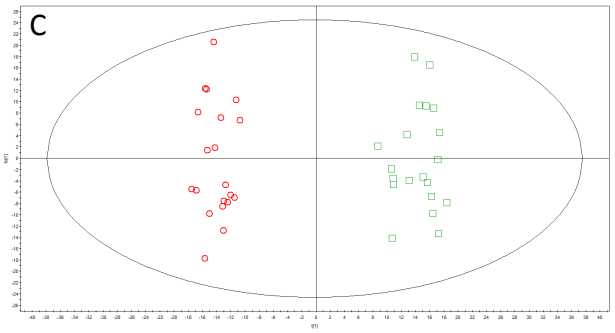

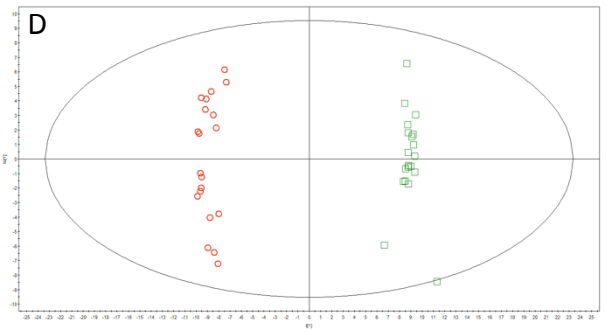

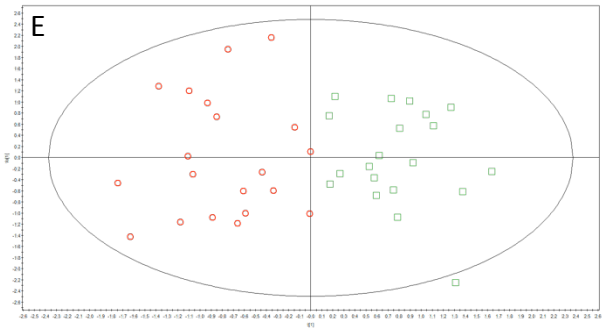

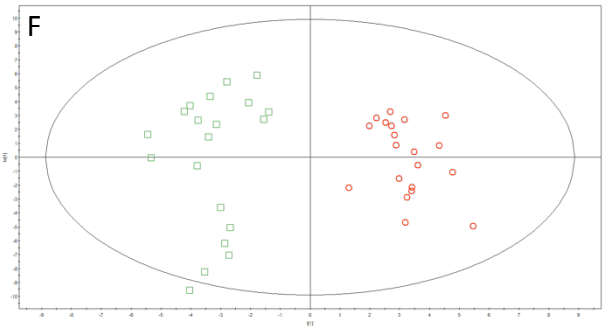

Figure 2

Click here to download Figure: Figure 2 new.pdf

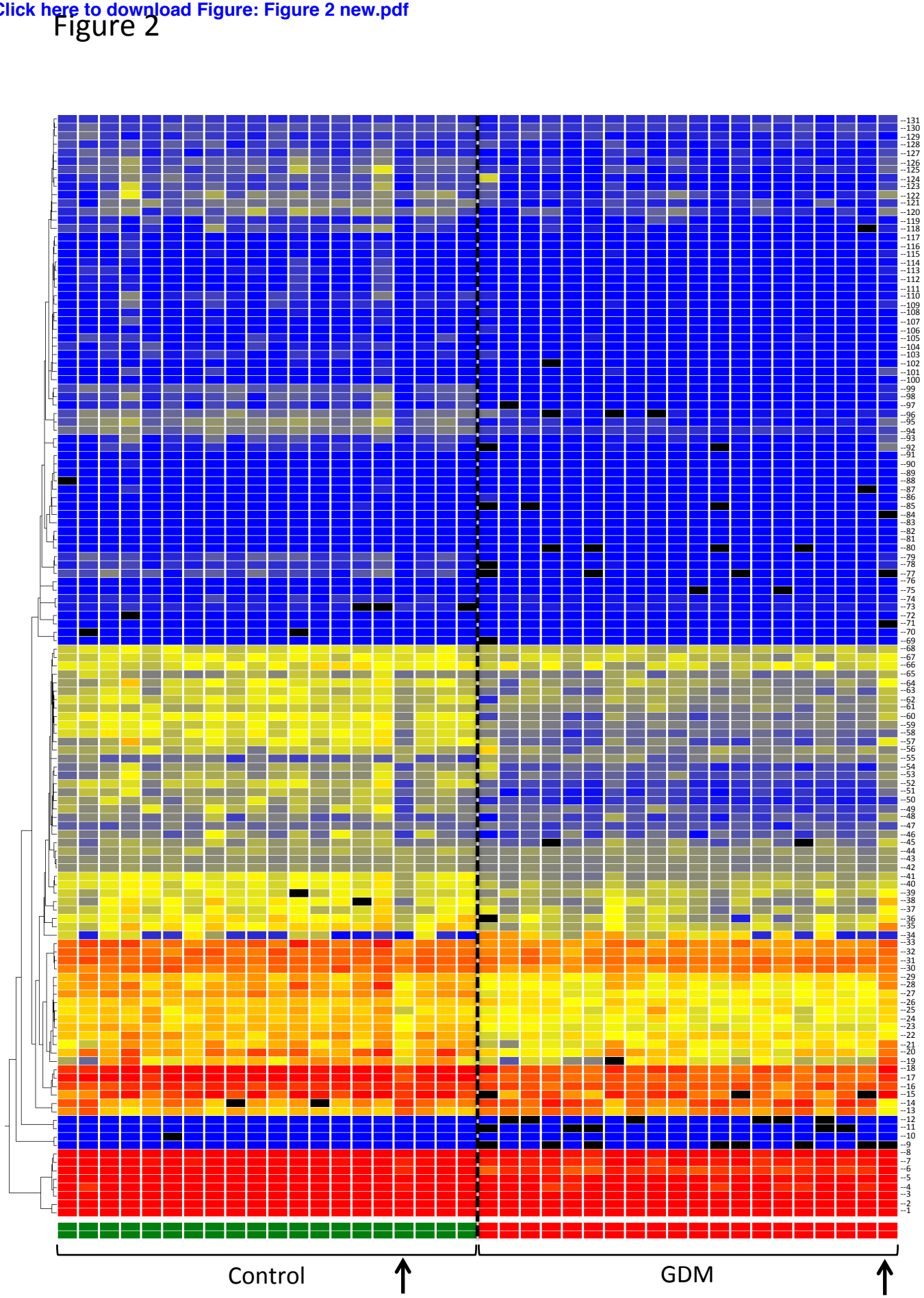

Figure 3
Figure 3
Click here to download Figure: Figure 3 color.pdf

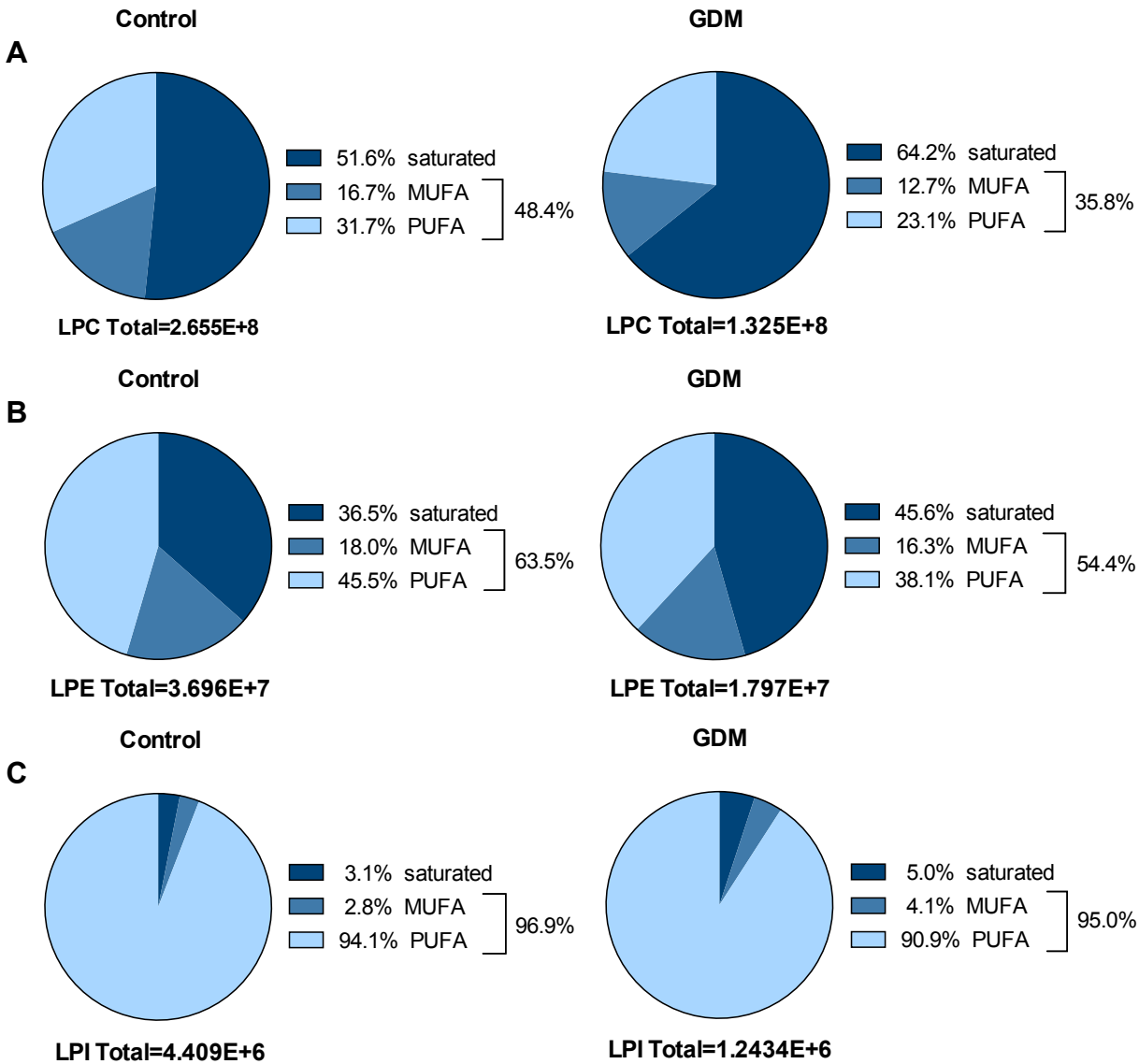

Figure 4

Figure 4

Click here to download Figure: Figure 4 color.pdf